Langmuir

Article

pubs.acs.org/Langmuir

Influence of Substrate Confinement on the Phase-Correlation in the Capillary Breakup of Arrays of Patterned Polymer Stripes

Zheng Zhang, Liang Wang, and Yifu Ding*

Department of Mechanical Engineering, University of Colorado, Boulder, Colorado 80309-0427, United States

Supporting Information

ABSTRACT: We investigated the influence of substrate confinement on the capillary breakup of parallel non-axisymmetric polymer stripes suspended on top of, or confined between, another immiscible polymer pattern. When the residual layer thickness of the pattern was reasonably large, the PS (or PMMA) stripes confined within PMMA (or PS) trenches broke up, either nucleated, out-of-phase, or without clear phase correlation depending on the geometry and viscosity ratio between the two polymers. In stark contrast, for the two extreme cases of viscosity ratios we studied, in-phase breakup of confined polymer stripes was always observed when the alternating PS/PMMA stripes were formed, that is, without residual layer, regardless of the specific geometry.

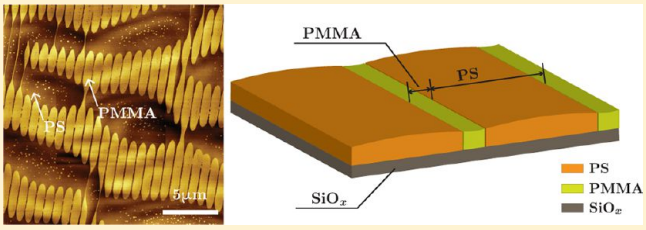

INTRODUCTION

The stability of nanostructured polymers depends on their viscoelastic properties and a range of surface and interfacial interactions particularly in the liquid state. Polymeric nanostructures and thin-films can spontaneously rupture into interesting structures upon heating via different mechanisms such as spinodal,[1] Marangoni[2] and nucleation-and-growth[3−5] instabilities. In the past, experimental efforts have been made to direct the structural/morphological evolution by using thermal gradient,[6,7] electrical field,[8,9] and topographically[10,11] or chemically[12,13] patterned substrates. The resultant hierarchical structures often times possess complexity beyond the capability of traditional top-down lithographic techniques.[14−17] Therefore, a thorough understanding of the mechanisms that dictate the structural evolution is important not only for manufacturing robust polymer nanostructures but also for utilizing the rupture processes to achieve useful structures.

Viscous polymer nanowires (or stripes) with large length-to-diameter (or width) ratios tend to rupture, driven by the capillary fluctuations at the surfaces and/or interfaces.[18,19] At a temperature above its glass transition temperature (T_g), a single cylindrical polymer thread embedded in an immiscible viscous liquid medium will break into isolated droplets to minimize the interfacial area. The average distance between neighboring droplets reflects the wavelength of the fastest-growing mode of fluctuation, which further depends on the initial thread diameter and the thread-to-medium viscosity ratio.[20] The simultaneous capillary breakup of multiple polymer threads has been investigated recently. When the threads are separated by rigid walls, each thread ruptures independently.[21,22] However, when an array of threads are embedded in an immiscible viscous liquid, strong hydrodynamic interactions can occur during the capillary breakup of the neighboring threads, resulting in phase-correlation between the final droplets.

The nature of the phase correlation can be manipulated by the diameter and lateral distance between neighboring threads, as well as the thread-to-medium viscosity ratio.[23−25] Specifically, in-phase breakup occurs when the threads are close to each other, in which case the necking/breaking locations of neighboring threads are aligned perpendicularly to the long axis of the threads. As the distance between neighboring threads increases, out-of-phase breakup occurs; the necking point of a thread forms next to a droplet of a neighboring thread. When the threads are sufficiently far away from their neighbors, no phase-correlation is expected.[23−25] Besides the fiber arrays studied, out-of-phase breakup was observed in the late stage of polymer blends demixing under shearing conditions.[26]

Significant suppression of capillary instability was observed when a polymer thread and the surrounding medium were contained within rigid confinement, either under quiescent[27,28] or pressure-driven flow[29] conditions. Son et al. found that confined threads tend to undulate parallel to the capping plates more than in the vertical direction, which resulted in squashed-ribbon shapes. This nonaxisymmetric shape provided stability against the amplification of interfacial fluctuations.[27,30] Accordingly, the breakup kinetics was slowed down when rigid confinement was imposed.[28] Recent theoretical work also indicated that the breakup wavelength, kinetics, and phase correlation can be dramatically modified under rigid confinement.[31]

Here, we study the influence of substrate confinement on the breakup behaviors of patterned submicrometer polymer stripes on top of, or separated by, another immiscible viscous polymer. We found that the capillary breakup of these confined polymer

Received: November 13, 2012
Revised: January 7, 2013
Published: February 8, 2013

   dx.doi.org/10.1021/la304528t | Langmuir 2013, 29, 3073−3079

stripes varied with the geometry and degree of substrate confinement. With the increase of confinement, the simultaneous breakup of the polymer stripes transitioned from either nucleation or out-of-phase mode to an in-phase mode, regardless of the preferential wetting of the components. Morphological evolution was consistent for the two extreme cases of stripe-to-medium viscosity ratios that were studied. A variety of arrays of droplets with different spatial arrangements can thus be obtained by manipulating these factors.

■ EXPERIMENTAL SECTION

Poly(methyl methacrylate) (PMMA) and polystyrene (PS) with a monodisperse molecular weight distribution were purchased from Polymer Source, Inc. Both polymers were used without further modification. Listed in Table 1 are the molecular weight, T_g, polydispersity index (M_w/M_n) and viscosity of both PS and PMMA. The values of T_g were determined from the second scan on a NETZSCH 204F1 differential scanning calorimeter (DSC), operated at a heating rate of 20 °C/min. The viscosities were calculated from previous literature.[32,33]

Table 1. Molecular Weight, T_g, Polydispersity Index (M_w/M_n) and Viscosity of the Polymers Used

polymer	M_w (g/mol)	T_g(°C)	M_w/M_n	η(Pa·s, @150 °C)	acronym
PS	17 700	89.2	1.04	1.9×10^3	PS17.7*k*
PMMA	16 700	110.4	1.06	5.4×10^5	PMMA16.7*k*

PS17.7*k*/toluene solutions of three different weight concentrations (1.0, 2.0, and 3.5 wt %) were first spin-coated onto 380 μm thick silicon substrates. The silicon substrates had been treated with piranha solutions and oxygen plasma prior to use, which resulted in a thin oxide layer at the surface. Immediately after spin-coating, the PS films were placed in a vacuum oven at 60 °C (below the T_g of PS17.7*k*) for 2 h in order to remove the remaining toluene.

Nanoimprint lithography (NIL) was used to replicate a surface grating pattern from a silicon mold onto the PS films, with an Eitre 3 (Obducat Inc.) nanoimprinter under a pressure of 4 MPa at 140 °C for 3 min. Since the molecular weight of PS used is well below its critical molecular weight for entanglement ($M_c \approx 35$ kg·mol^{-1} for bulk PS),[32] the experimental time-scale of the imprinting process was long enough to allow residual stresses to fully relax.[34,35] Therefore, we do not expect strong residual stress effects resulted from the nanoimprinting during the capillary breakup of the stripes discussed below. A silicon mold containing line grating patterns, with a pattern height of 240 nm, a periodicity of 834 nm and a line-to-space ratio of 1, was used for patterning all samples. To facilitate releasing the mold from the imprinted PS films at room temperature, a silanizing agent (tridecafluoro-1,1,2,2-tetrahydrooctyl trichlorosilane, purchased from Sigma-Aldrich, Inc. and used as received) was deposited on the surface of the mold via vapor deposition, which would reduce the adhesion between the PS and the silicon mold.[36]

PMMA16.7*k* was subsequently spin-coated onto the imprinted PS patterns from an acetic acid (a selective solvent for PMMA[37] that does not dissolve PS) solution with a weight concentration of 1 wt %. The resultant bilayer-type patterns were again annealed in a vacuum oven at 60 °C (below the T_g of both PMMA16.7*k* and PS17.7*k*) for 2 h to remove residual solvents. The PMMA/PS bilayer samples were annealed under ambient conditions on an STC200 hot-stage (Instec, Inc.) with a temperature stability of 0.1 °C. Before use, the hot-stage had been calibrated for the temperature range of 47 to 286 °C, with 7 different melting point standards from Sigma-Aldrich, Inc. A Dimension 3100 atomic force microscope (AFM, Bruker Corp.) was operated under tapping mode for examining the morphological evolution induced by annealing, after the samples had been cooled down to room temperature. Silicon probes with resonant frequencies of approximately 300 kHz and spring constants ranging from 25 to 75 N/m were used for all AFM measurements. In addition to PMMA/PS bilayer samples, PS on PMMA patterns (PS/PMMA) were also prepared and characterized with similar protocols. Furthermore, the PMMA (or PS) was selectively dissolved with acetic acid (or cyclohexane) exposing the original PMMA/PS interface for characterization with AFM, as well as a JEOL JSM-7401F field emission scanning electron microscope (FE-SEM).

■ RESULTS AND DISCUSSION

Recently, we reported the instabilities of patterned multiple PS stripes aligned in parallel on PMMA line-and-space patterns with a thick residual layer, when annealed at temperatures above the T_g of both polymers.[38,39] The thickness of the

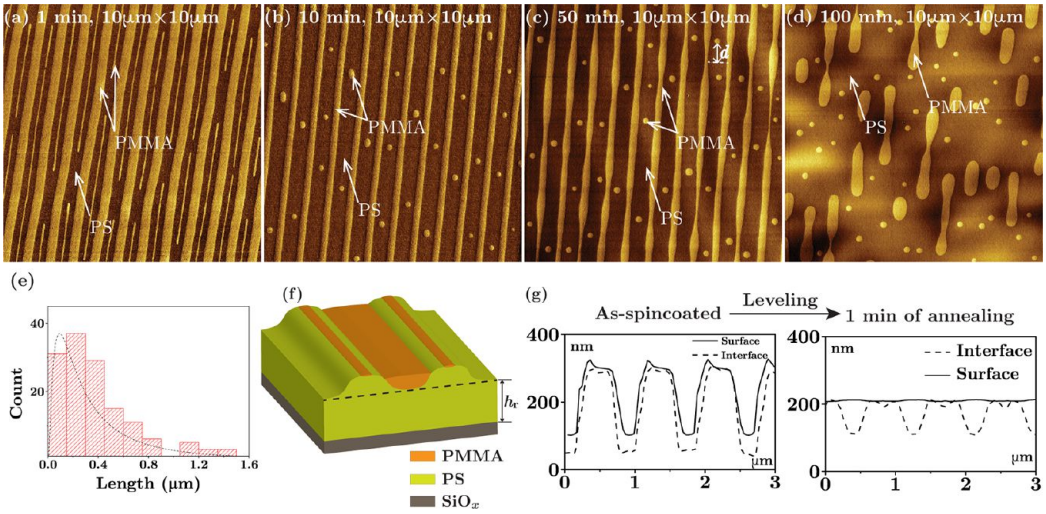

Figure 1. (a−d) AFM phase images of the PMMA1%/PS3.5% sample after annealing at 150 °C for different amounts of time, as specified at the upper left corner of each image. The scan-sizes for all four images are 10 μm × 10 μm. (e) A statistical histogram of the distance, *d*, along line direction, between a small droplet and its nearest stripe-necking spot, for the annealing duration of 50 min (schematically shown in (c)). A total number of 141 small droplets have been counted. (f) A schematic for the cross-section after 1 min of annealing, as shown in (a). (g) Cross-sectional height profiles change during the surface-tension-induced leveling process. The AFM height images and profiles for (a−d) are provided in Figure S5 of the Supporting Information.

residual layer *after* the surface-leveling process (discussed below) is specifically defined as h_r in part f of Figure 1. Briefly, we found that the PS stripes underwent a two-stage capillary instability atop PMMA patterns during annealing: narrower ones on the PMMA mesa broke up first, followed by the out-of-phase breakup of the larger ones confined in the PMMA trenches. The dependence of the wavelength and kinetics on the viscosity ratio of PS/PMMA was examined systematically. For that system, the PMMA layer wet the SiO_x surface of the substrate and h_r was larger than 150 nm during the capillary breakup of the PS stripes. Here, we mainly focus on understanding the influence of the substrate confinement, that is, with small or zero h_r, on the capillary breakup of the patterned arrays. To examine whether the preferential wetting of PS/PMMA on the substrate played a role, we studied both PS cast on PMMA patterns and PMMA on PS patterns. In the following, we focus on describing the PMMA cast on imprinted PS patterns first.

The PS film thickness, cast from a 3.5 wt % toluene solution, was ∼170 nm, which resulted in a residual layer thickness of ∼50 nm in the imprinted PS pattern (the distance between the PS grooves and the SiO_x substrate), determined by the mold geometry. AFM measurement confirmed faithful replication of the patterns from the mold onto the PS film (part a1 of Figure S6 of the Supporting Information). PMMA16.7*k* was then spin-coated onto the imprinted PS films out of an acetic acid solution with a concentration of 1 wt %. Most PMMA was deposited within the trenches of the PS pattern, with a smaller amount left on top of the PS mesas. Therefore, the total amplitude of the pattern decreased, as shown in part g of Figure 1. The as-imprinted PS pattern was ∼240 nm tall and the overall pattern height reduced to ∼198 nm after the PMMA deposition. The corrugation of the PMMA layer was found to be in-phase with the underlying PS pattern, which was consistent with Mukherjee et al.[40] Furthermore, according to Roy et al., the PMMA should have formed a continuous layer.[41] The surface morphology of the resultant bilayer system is shown in part a2 of Figure S6 of the Supporting Information.

Upon annealing at 150 °C, which was above the T_g of both polymers, the morphology of the PMMA/PS pattern started to evolve (Figure 1 and Figure S5 of the Supporting Information). As detailed in the Experimental Section, adequate heating time allowed the residual stresses, imposed by spin-coating and the NIL process, to relax.[34,35] Therefore, the onset of the instabilities was *not* induced by residual stresses. At the very early stage, surface-tension-driven pattern leveling was dominant, causing the surface of the pattern to smooth out. After only 1 min, the overall PMMA/PS pattern height reduced from 198 nm to ∼6 nm (parts a1 and a2 of Figure S5 of the Supporting Information). Meanwhile, PMMA was segregated into two sets of parallel stripes, narrower ones on top of the PS mesas, and wider ones within the PS trenches (part a of Figure 1). This process was driven by the tendency of PMMA to reach the equilibrium Neumann contact angle with PS, which was dictated by the balance between the PMMA surface tension and the PS/PMMA interfacial tension.[39] Part g of Figure 1 shows the overall geometrical changes during the leveling process. The 3D view of this complex PS/PMMA pattern is schematically shown in part f of Figure 1. As discussed in our previous report, the equilibrium shapes of the PMMA stripes were not cylindrical and were determined by the balance of Laplace pressure between the PMMA surface and PS/PMMA interface.[39]

The narrower PMMA stripes, centered on the PS mesas, had an average width of ∼70 nm and a thickness of ∼20 nm. The geometry of these stripes was only transient as they started to break up due to capillary fluctuations almost as soon as they formed (part a of Figure 1). There appeared no phase-correlation for the necking/breaking locations between the neighboring PMMA stripes. This was simply because the lateral distance-to-width ratio of the stripes (nearly 20:1) was so large that the hydrodynamic interactions among neighboring narrow PMMA stripes was negligible.[24] After 10 min, the narrow stripes have completely broken into aligned PMMA droplets on top of the PS mesas confined between the wider PMMA stripes (part b of Figure 1). The average distance between two adjacent droplets along the original line direction was measured to be 3.3 ± 0.8 μm.

During this period, the wider PMMA stripes within the PS trenches remained unbroken. Their widths shrank to ∼300 nm from originally 417 nm, whereas their thicknesses increased to ∼125 nm, as determined from AFM measurements after selectively removing the PMMA with acetic acid. At this stage, h_r of the PS pattern became 100 nm. Such a cross-sectional profile of the suspended PMMA stripes was determined by the balance between the surface tension of PMMA and the PS-PMMA interfacial tension.[39] Up to this point, the overall morphological changes of the PMMA/PS pattern were similar to that of the PS/PMMA pattern reported recently.[39]

After 50 min, undulation along the long axes of the PMMA stripes, associated with the capillary fluctuations, was clearly observed, and isolated droplets formed after 100 min (parts c and d of Figure 1). Interestingly, the locations of these necking/pinching-off points along the PMMA stripes were clearly different from that of the PS/PMMA bilayer pattern reported in ref 39. In PS/PMMA system, the PS stripes in PMMA trenches dominantly broke up in an out-of-phase fashion. In contrast, the necking/pinching-off of the PMMA stripes reported here appeared more likely to occur around the smaller PMMA droplets resulted from the breakup of smaller PMMA stripes on the PS mesas (part c of Figure 1). Such a correlation is more evident in part d of Figure 1, which shows that most of the smaller PMMA droplets accumulated in the vicinity of the necked regions between the larger PMMA droplets. Because of the self-assembly nature of the morphological evolution, we do not expect this observation to be exact for *all* the droplets.

To examine whether this correlation is statistically significant (against the randomness in this self-assembly process), we analyzed the positions of 141 small PMMA droplets from multiple AFM scans at different locations across the sample surface (annealed for 50 min). The distance along the stripe direction, d (illustrated in part c of Figure 1), between the position of a small droplet and that of the nearest necking spots of the large PMMA stripes, was determined for all the 141 droplets. The distribution of the d is shown in part e of Figure 1, revealing that a majority of the droplets were found to be within 0.4 μm away from the necking spots, which was 8 times smaller than the average distance between droplets. Such a nucleation-like breakup of the PMMA stripes in the vicinity of smaller PMMA droplets was not observed in the PS stripes on the PMMA patterns (ref 39). This discrepancy was caused by the much stronger hydrodynamic effect in the present system: both the size of the droplets and the droplet/medium viscosity ratio were much larger in the present system.

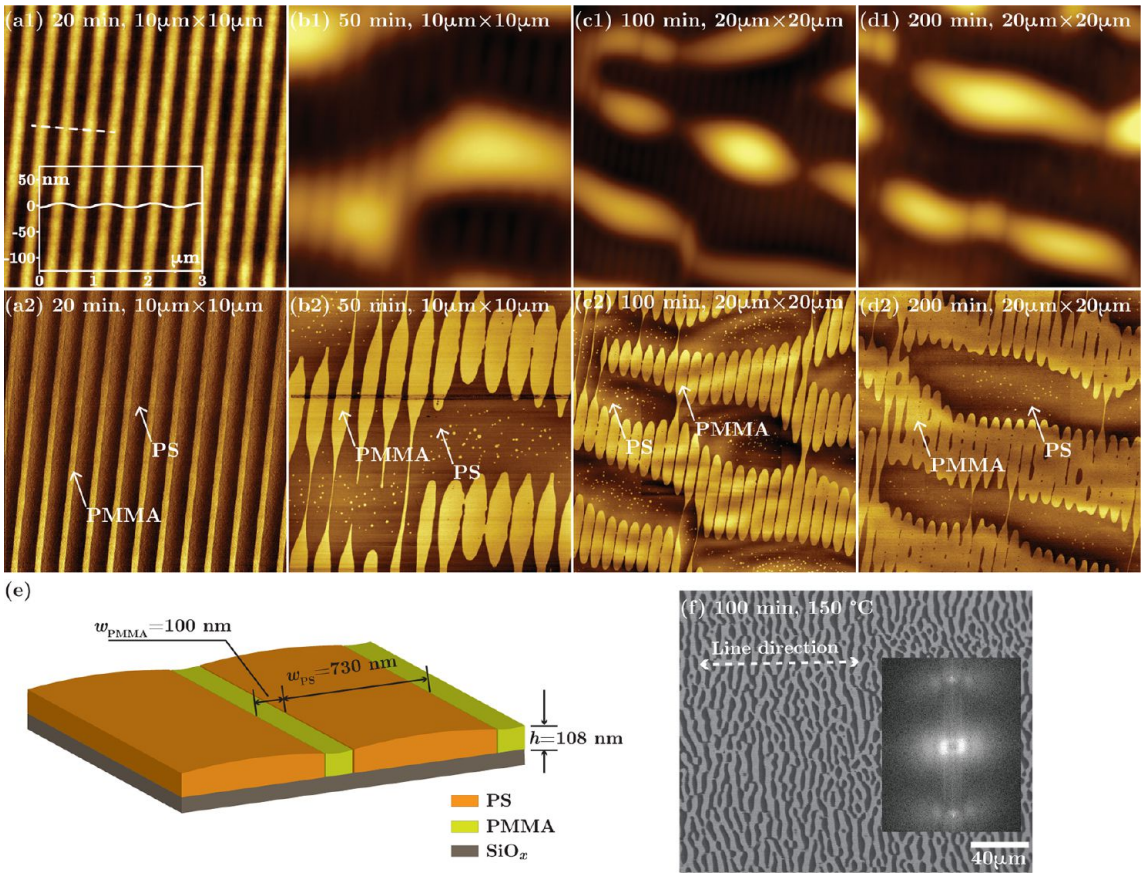

Figure 2. (a1−d1) AFM topographic images and (a2−d2) their corresponding phase images of the PMMA1%/PS2% sample after being annealed at 150 °C for different amounts of time, as specified at the upper left corner of each image. The insert of (a1) is the line profile for the area marked with a dashed line. (e) A schematic for the cross-sectional geometry of (a1). (f) Field-emission SEM image of the sample surface after annealing at 150 °C for 100 min and selectively dissolving PMMA. The original line direction is marked with the dashed arrow. Insert of (f) is a fast Fourier transformation (FFT) of the SEM image.

After annealing for 100 min, larger PMMA droplets and blocks of PMMA stripes were observed, which completely ruptured into droplets after 250 min (Figure S1 of the Supporting Information). Thus, a bimodal-like distribution of PMMA droplets within a continuous PS film was obtained. The smaller PMMA droplets started migrating, which was driven by the flow field associated with the breakup of the larger PMMA stripes. Upon further annealing, the morphological evolution of the film was dominated by both the coarsening and substrate-wetting of the PMMA droplets, which induced significant roughening of the entire films (Figure S2 of the Supporting Information).

To impose strong substrate-induced confinement effect, PMMA stripes partially confined on PS patterns with ultrathin (or negligible) residual layers were prepared. This was achieved by reducing the thickness of the as-cast PS film (Figure S4 of the Supporting Information, which characterizes the thickness of the residual layer). Bogdanski et al. showed that a negligible residual layer could be achieved by the incomplete filling of molds, where direct lift-off was successful without any etching.[42,43] Specifically, a 90 nm and a 55 nm PS films were prepared by spin-coating from 2% and 1% toluene solutions. For the 90 nm film, the as-imprinted PS pattern showed a residual layer thickness of ∼9 nm, as determined by the AFM measurements on a scratched pattern. In comparison, no residual layer was observed for the PS pattern imprinted from the 55 nm films. Subsequently, PMMA was deposited on top of the PS patterns by spin-coating from a 1% acetic acid solution. Upon annealing, the morphological evolution of the two PMMA/PS patterns were similar. In the following, we focus on discussing the sample prepared from the 90 nm PS film, and that from the 55 nm is presented in Figure S3 of the Supporting Information.

Figure 2 shows the morphological evolution of the PMMA1%/PS2% sample during annealing at 150 °C. Similar to all the previous samples, surface-tension driven leveling dominated the early stage of the pattern evolution, resulting in a rather smooth PMMA/PS pattern by 20 min, with a root-mean-square (RMS) roughness of 2.9 nm (insert of part a1 of Figure 2). Alternating stripes of PMMA and PS formed, as indicated by the arrows in part a2 of Figure 2. After selectively removing PMMA (with acetic acid) or PS (with cyclohexane), the geometries of the PMMA/PS pattern were determined (Figure S4 of the Supporting Information for the method used to determine the cross-sectional geometry). As schematically illustrated in part e of Figure 2, both PS and PMMA formed direct contact with the Si substrate, with an average line height (h) ∼108 nm. The width of the PMMA stripes (w_{PMMA}) was ∼100 nm while that of the PS (w_{PS}) was ∼730 nm.

After 50 min, The PMMA stripes broke up and formed droplets, while PS stripes merged into a continuous film, as shown parts b1 and b2 of Figure 2. Most significantly, the positions of the PMMA droplets clearly showed that the breakup of the PMMA stripes occurred via an in-phase mode,

with the droplets and necking positions lined up across neighboring stripes. This is in stark contrast to the system with a 70 nm residual layer discussed in Figure 1. After the necking had occurred, the width of the PMMA blocks increased due to the contraction along the length direction. As a result, the area coverage of PMMA increased from ∼12% in part a2 of Figure 2 to ∼37% in part b2 of Figure 2 because of the preferential wetting of PMMA on SiO_x. This preferential wetting of PMMA forced the PS to deform out-of-plane and caused significant roughening of the film with an RMS roughness ∼60 nm (part b1 of Figure 2). Further annealing caused the PS blocks to start to contract in length (parts c1 and c2 of Figure 2) and form a larger stripe-like structure in the direction perpendicular to the original lines, as shown in part f of Figure 2 over a larger area. From the FFT image in part f of Figure 2, the most significant correlation length between the PS blocks was 6.5 μm. Recent theoretical work showed that confinement moderately affects the breakup wavelength.[31] However, a quantitative understanding of the wavelength for such complex nonaxisymmetric stripes with three different surface/interfacial energies is currently lacking.

With increasing amount of annealing time, more merging/coarsening of the PMMA blocks were evident (part d2 of Figure 2). The underlying mechanism might be collision-induced coarsening. However, the PS thin lines trapped between the PMMA blocks prevented them coarsening into more rounded shapes. Parts b2−d2 of Figure 2 also showed that some of the thin ligands connecting two broken PMMA blocks did not rupture even after 200 min. The slowed rupture kinetics might be because that the elastic stresses developed during thinning were able to balance the capillary forces.[44]

For this system, both PMMA and PS stripes were in contact with the rigid Si substrate, which inhibited deformation into the substrate.[45,46] Therefore, the lateral flow/deformation of the PMMA stripes were highly correlated with that of the PS stripes. An in-phase rupture of the PMMA stripes indicated that the PS stripes should also show in-phase fluctuations, that is, the increase (decrease) of PMMA width in the stripes was accompanied by the decrease (increase) of the contacting PS stripes (part b2 of Figure 2). Apparently, the PMMA stripes broke/pinched off quicker than the PS stripes, probably due to its much smaller original width (part e of Figure 2).

To further examine the generality of the observed simultaneous capillary breakup in the confined polymer stripes, PMMA1%/PS1% were examined. As mentioned above, the as-imprinted PS pattern did not show any detectable residual layer. After annealing at 150 °C for 50 min, alternating PS and PMMA stripes formed after the surface-leveling, similar to that shown in part e of Figure 2. The geometries of the cross sections of the stripes were: with w_{PS} = 500 nm, w_{PMMA} = 330 nm, and h = 81 nm, as schematically drawn in Figure S3 of the Supporting Information. The PS to PMMA volume ratio was estimated to be 1.5, much smaller than that shown in part e of Figure 2. Similar in-phase simultaneous capillary breakup was observed, with the only difference being that isolated PS droplets formed instead of PMMA (Figure S3 of the Supporting Information vs Figure 2). This discrepancy was most likely attributed to the fact that the time scale of necking/pinching-off of the PS stripes was shorter compared with the PMMA ones, as their widths were comparable but PMMA was more viscous. The wavelength, or correlation length, of the droplets formed was ∼5.6 μm.

Furthermore, we examined the PS/PMMA system, by casting PS (0.5% toluene solution) on nanoimprinted PMMA patterns. PMMA patterns with a residual layer thickness of ∼50 nm were imprinted from a film cast from 2.5% acetic acid solution. After the surface leveling upon annealing at 150 °C for 5 min, PS stripes confined within PMMA trenches were obtained (part a of Figure 3), which subsequently broke up without a clear phase correlation between the neighboring stripes (part b of Figure 3). Note that there were indeed tiny PS droplets (diameter <50 nm) on the PMMA mesa, but they did not affect the breakup of the larger PS stripes because they were too small. In comparison, the as-imprinted PMMA patterns prepared on thinner film, cast from a 1.5% acetic acid solution, showed a residual layer thickness of less than 5 nm. In this case, alternating PS/PMMA stripes formed after surface leveling upon annealing at 150 °C, which broke up subsequently via an in-phase mode (part d of Figure 3), similar to that observed in Figure 2 and Figure S3 of the Supporting Information. The correlation length of the PS droplets, along the original line direction, was around 4.2 μm. Interestingly, satellite (smaller) PS droplets between the larger ones were observed in part d of Figure 3, a morphology that is different from that observed in part b2 of Figure 2 and Figure S3 of the Supporting Information. The formation of such satellite or secondary droplets is attributed to the larger width and lower viscosity of the PS stripes, which is a phenomenon also observed in the capillary breakup of fluid filaments with low viscosity.[47]

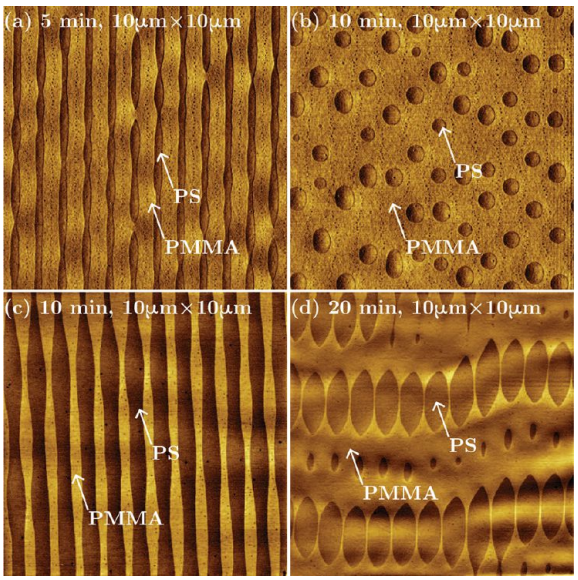

Figure 3. AFM phase images of (a, b) PS0.5%/PMMA2.5% and (c, d) PS0.8%/PMMA1.5%, after being annealed at 150 °C for the labeled durations.

From literature, simultaneous in-phase breakup of multiple threads (with unperturbed radius r) often occurs at small center-to-center distance (d). Therefore, reducing the distance between the threads should always favor in-phase. For example, when the thread-to-medium viscosity ratio approaches 1, the critical distance, d/r, below which in-phase breakup occurs, is around 3.[24,25] Furthermore, when the thread-to-medium viscosity ratio is below 0.25, no in-phase breakup is expected.[31] From the aforementioned experimental results, it is clear that increasing the substrate confinement, or decreasing the residual layer thickness, indeed leads to in-phase breakup of the

patterned polymer stripes, regardless of the viscosity ratio between the two polymers.

Once the alternating PS/PMMA stripes were developed, in-phase breakup of either PS or PMMA stripes was always observed, even though the two extreme cases of viscosity ratios between the broken stripes to the unbroken ones differed by several orders of magnitude. Furthermore, the ratio between the center-to-center distance of the neighboring stripes (equals the pitch of the pattern, 834 nm) and the width of the broken stripes ranged from ∼2 (Figure 3) to more than 10 (Figure 1). However, the collective wavelength of the in-phase breakup was comparable for all the experiments (Figures 2 and 3 and Figure S3 of the Supporting Information). Therefore, the in-phase breakup observed in the confined polymer stripes here was dictated by different hydrodynamic scaling, if any, from what was found in fully embedded polymer threads.[24]

■ CONCLUSIONS

In this study, we investigated the influence of substrate confinement on the capillary breakup of parallel noncylindrical polymer stripes suspended on top of, or confined between, another immiscible polymer pattern. Prior to the capillary breakup, a surface-tension-induced leveling was observed for all samples. When the residual layer thickness was reasonably large, the PS (or PMMA) stripes confined within PMMA (or PS) trenches broke up, either nucleated (Figure 1), out-of-phase (ref 39), or without clear phase correlation (part b of Figure 3) depending on the geometry and viscosity ratio between the stripes and medium. Most significantly, in-phase breakup of the confined polymer stripes were always observed when, preceding capillary breakup, alternating PS/PMMA stripes were formed, that is, without residual layer. The in-phase breakup was caused by the rigid substrate confinement effect, because when the bottom layer was thin, the polymer interface would become less deformable.[45,46] Therefore, the viscous deformation was forced in-plane, in which case the necking of neighboring stripes became strongly coupled in an in-phase manner. A critical as-imprinted residual layer thickness of less than ∼10 nm was experimentally found, below which in-phase breakup would occur, in the two extreme cases of stripe-to-medium viscosity ratios we studied (280/1 and 1/280). The preferential wetting of the polymer components was not found to affect the morphological evolution during the annealing duration that we examined.

These experimental findings call for theoretical work that can describe the capillary breakup of nonaxisymmetric polymer threads, as well as the phase correlation between these multiple stripes. Nevertheless, controlling the breakup behaviors of the bilayer-like polymer patterns can thus provide a pathway to creating a plethora of hierarchical structures in thin polymer films by adjusting the geometry and properties of both polymers.

■ ASSOCIATED CONTENT

Supporting Information

AFM phase and height images. This material is available free of charge via the Internet at http://pubs.acs.org.

■ AUTHOR INFORMATION

Corresponding Author

*E-mail: Yifu.Ding@Colorado.edu.

Notes

The authors declare no competing financial interest.

■ ACKNOWLEDGMENTS

The authors acknowledge the funding support from the National Science Foundation under Grant No. CMMI-1031785. Acknowledgement is made to the donors of the Petroleum Research Fund, administered by the American Chemical Society, for partial support of this research (Grant Number: ACS-PRF 50581-DNI7).

■ REFERENCES

(1) Xie, R.; Karim, A.; Douglas, J. F.; Han, C. C.; Weiss, R. A. Spinodal dewetting of thin polymer films. *Phys. Rev. Lett.* **1998**, *81*, 1251−1254.

(2) Nepomnyashchy, A. A.; Simanovskii, I. B. Marangoni instability in ultrathin two-layer films. *Phys. Fluids* **2007**, *19*, 122103−122103−14.

(3) Reiter, G. Dewetting of thin polymer films. *Phys. Rev. Lett.* **1992**, *68*, 75−78.

(4) Reiter, G. Unstable thin polymer films: Rupture and dewetting processes. *Langmuir* **1993**, *9*, 1344−1351.

(5) Stange, T. G.; Evans, D. F.; Hendrickson, W. A. Nucleation and growth of defects leading to dewetting of thin polymer films. *Langmuir* **1997**, *13*, 4459−4465.

(6) Schäffer, E.; Harkema, S.; Roerdink, M.; Blossey, R.; Steiner, U. Morphological instability of a confined polymer film in a thermal gradient. *Macromolecules* **2003**, *36*, 1645−1655.

(7) Nepomnyashchy, A.; Simanovskii, I. Instabilities and ordered patterns in nonisothermal ultrathin bilayer fluid films. *Phys. Rev. Lett.* **2009**, 102.

(8) Schäffer, E.; Thurn-Albrecht, T.; Russell, T. P.; Steiner, U. Electrically induced structure formation and pattern transfer. *Nature* **2000**, *403*, 874−877.

(9) Morariu, M. D.; Voicu, N. E.; Schäffer, E.; Lin, Z.; Russell, T. P.; Steiner, U. Hierarchical structure formation and pattern replication induced by an electric field. *Nat. Mater.* **2002**, *2*, 48−52.

(10) Higgins, A. M.; Jones, R. A. L. Anisotropic spinodal dewetting as a route to self-assembly of patterned surfaces. *Nature* **2000**, *404*, 476−478.

(11) Herminghaus, S.; Brinkmann, M.; Seemann, R. Wetting and dewetting of complex surface geometries. *Annu. Rev. Mater. Res.* **2008**, *38*, 101−121.

(12) Rockford, L.; Liu, Y.; Mansky, P.; Russell, T. P.; Yoon, M.; Mochrie, S. G. J. Polymers on nanoperiodic, heterogeneous surfaces. *Phys. Rev. Lett.* **1999**, *82*, 2602−2605.

(13) Sehgal, A.; Ferreiro, V.; Douglas, J. F.; Amis, E. J.; Karim, A. Pattern-directed dewetting of ultrathin polymer films. *Langmuir* **2002**, *18*, 7041−7048.

(14) Krausch, G. Surface induced self assembly in thin polymer films. *Materials Science and Engineering: R: Reports* **1995**, *14* (v−vi), 1−94.

(15) Geoghegan, M.; Krausch, G. Wetting at polymer surfaces and interfaces. *Prog. Polym. Sci.* **2003**, *28*, 261−302.

(16) Hamley, I. Ordering in thin films of block copolymers: Fundamentals to potential applications. *Prog. Polym. Sci.* **2009**, *34*, 1161−1210.

(17) Xue, L.; Han, Y. Pattern formation by dewetting of polymer thin film. *Prog. Polym. Sci.* **2011**, *36*, 269−293.

(18) Rayleigh, L. On the instability of cylindrical fluid surfaces. *Philos. Mag.* **1892**, *34*, 177.

(19) Rayleigh, L. On the instability of a cylinder of viscous liquid under capillary force. *Philos. Mag.* **1892**, *34*, 145.

(20) Tomotika, S. On the instability of a cylindrical thread of a viscous liquid surrounded by another viscous fluid. *Proc. Royal Soc. London, Ser. A* **1935**, *150*, 322−337.

(21) Suh, K. Y.; Lee, H. H. Anistropic hole formation in thin polymer films confined by walls. *J. Chem. Phys.* **2001**, *115*, 8204−8208.

(22) Suh, K.; Lee, H. Capillary force lithography: Large-area patterning, self-organization, and anisotropic dewetting. *Adv. Funct. Mater.* **2002**, *12*, 405−413.
(23) Elemans, P. H. M.; van Wunnik, J. M.; van Dam, R. A. Development of morphology in blends of immiscible polymers. *AIChE J.* **1997**, *43*, 1649−1651.
(24) Knops, Y. M. M.; Slot, J. J. M.; Elemans, P. H. M.; Bulters, M. J. H. Simultaneous breakup of multiple viscous threads surrounded by viscous liquid. *AIChE J.* **2001**, *47*, 1740−1745.
(25) Gunawan, A.; Molenaar, J.; van de Ven, A. In-phase and out-of-phase break-up of two immersed liquid threads under influence of surface tension. *Eur. J. Mechanics - B/Fluids* **2002**, *21*, 399−412.
(26) Martys, N. S.; Douglas, J. F. Critical properties and phase separation in lattice Boltzmann fluid mixtures. *Phys. Rev. E* **2001**, *63*, 031205.
(27) Son, Y.; Martys, N. S.; Hagedorn, J. G.; Migler, K. B. Suppression of capillary instability of a polymeric thread via parallel plate confinement. *Macromolecules* **2003**, *36*, 5825−5833.
(28) Hagedorn, J. G.; Martys, N. S.; Douglas, J. F. Breakup of a fluid thread in a confined geometry: Droplet-plug transition, perturbation sensitivity, and kinetic stabilization with confinement. *Phys. Rev. E* **2004**, *69*, 056312.
(29) Humphry, K. J.; Ajdari, A.; Fernández-Nieves, A.; Stone, H. A.; Weitz, D. A. Suppression of instabilities in multiphase flow by geometric confinement. *Phys. Rev. E* **2009**, *79*, 056310.
(30) San Miguel, M.; Grant, M.; Gunton, J. D. Phase separation in two-dimensional binary fluids. *Phys. Rev. A* **1985**, *31*, 1001−1005.
(31) Janssen, P. J. A.; Meijer, H. E. H.; Anderson, P. D. Stability and breakup of confined threads. *Phys. Fluids* **2012**, *24*, 012102.
(32) Majeste, J.-C.; Montfort, J. P.; Allal, A.; Marin, G. Viscoelasticity of low molecular weight polymers and the transition to the entangled regime. *Rheol. Acta* **1998**, *37*, 486−499.
(33) Fuchs, K.; Friedrich, C.; Weese, J. Viscoelastic properties of narrow-distribution poly(methyl methacrylates). *Macromolecules* **1996**, *29*, 5893−5901.
(34) Ding, Y.; Ro, H. W.; Douglas, J. F.; Jones, R. L.; Hine, D. R.; Karim, A.; Soles, C. L. Polymer viscoelasticity and residual stress effects on nanoimprint lithography. *Adv. Mater.* **2007**, *19*, 1377−1382.
(35) Ding, Y.; Ro, H. W.; Germer, T. A.; Douglas, J. F.; Okerberg, B. C.; Karim, A.; Soles, C. L. Relaxation behavior of polymer structures fabricated by nanoimprint lithography. *ACS Nano* **2007**, *1*, 84−92.
(36) Jung, G.-Y.; Li, Z.; Wu, W.; Chen, Y.; Olynick, D. L.; Wang, S.-Y.; Tong, W. M.; Williams, R. S. Vapor-phase self-assembled monolayer for improved mold release in nanoimprint lithography. *Langmuir* **2005**, *21*, 1158−1161.
(37) Walheim, S.; Böltau, M.; Mlynek, J.; Krausch, G.; Steiner, U. Structure formation via polymer demixing in spin-cast films. *Macromolecules* **1997**, *30*, 4995−5003.
(38) Ahn, D. U.; Wang, Z.; Yang, R.; Ding, Y. Hierarchical polymer patterns driven by capillary instabilities at mobile and corrugated polymer-polymer interfaces. *Soft Matter* **2010**, *6*, 4900−4907.
(39) Zhang, Z.; Ahn, D. U.; Ding, Y. Instabilities of PS/PMMA bilayer patterns with a corrugated surface and interface. *Macromolecules* **2012**, *45*, 1972−1981.
(40) Mukherjee, R.; Pangule, R. C.; Sharma, A.; Banerjee, I. Contact instability of thin elastic films on patterned substrates. *J. Chem. Phys.* **2007**, *127*, 064703−064703−6.
(41) Roy, S.; Ansari, K. J.; Jampa, S. S. K.; Vutukuri, P.; Mukherjee, R. Influence of substrate wettability on the morphology of thin polymer films spin-coated on topographically patterned substrates. *ACS Appl. Mater. Interfaces* **2012**, *4*, 1887−1896.
(42) Bogdanski, N.; Wissen, M.; Ziegler, A.; Scheer, H.-C. Temperature-reduced nanoimprint lithography for thin and uniform residual layers. *Microelectron. Eng.* **2005**, *78*−*79*, 598−604.
(43) Bogdanski, N.; Wissen, M.; Möllenbeck, S.; Scheer, H.-C. Thermal imprint with negligibly low residual layer. *J. Vac. Sci. Technol., B: Microelectron. Nanometer Struct.* 2006, *24*, 2998−3001.
(44) Tirtaatmadja, V.; McKinley, G. H.; Cooper-White, J. J. Drop formation and breakup of low viscosity elastic fluids: Effects of molecular weight and concentration. *Phys. Fluids* **2006**, *18*, 043101.
(45) Xu, L.; Bandyopadhyay, D.; Shi, T.; An, L.; Sharma, A.; Joo, S. W. Dewetting kinetics of thin polymer bilayers: Role of under layer. *Polymer* **2011**, *52*, 4345−4354.
(46) Xu, L.; Bandyopadhyay, D.; Sharma, A.; Joo, S. W. Switching of interfacial instabilities from the liquid/air interface to the liquid/liquid interface in a polymer bilayer. *Soft Matter* **2011**, *7*, 8056−8066.
(47) Wagner, C.; Amarouchene, Y.; Bonn, D.; Eggers, J. Droplet detachment and satellite bead formation in viscoelastic fluids. *Phys. Rev. Lett.* **2005**, *95*, 164504.